

Published in final edited form as:

*Nano Lett.* 2011 February 9; 11(2): 746–750. doi:10.1021/nl1038874.

## Controlled translocation of individual DNA molecules through protein nanopores with engineered molecular brakes

Marcela Rincon-Restrepo<sup>1,2</sup>, Ellina Mikhailova<sup>1</sup>, Hagan Bayley<sup>1</sup>, and Giovanni Maglia<sup>1,3</sup>

<sup>1</sup>Department of Chemistry, University of Oxford, Oxford, OX1 3TA, United Kingdom

### Abstract

Protein nanopores may provide a cheap and fast technology to sequence individual DNA molecules. However, the electrophoretic translocation of ssDNA molecules through protein nanopores has been too rapid for base identification. Here, we show that the translocation of DNA molecules through the  $\alpha$ -hemolysin protein nanopore can be slowed controllably by introducing positive charges into the lumen of the pore by site directed mutagenesis. Although the residual ionic current during DNA translocation is insufficient for direct base identification, we propose that the engineered pores might be used to slow down DNA in hybrid systems, e.g. in combination with solid-state nanopores.

### Keywords

alpha-hemolysin; DNA sequencing; nanopore; protein engineering; DNA translocation

The ability to sequence the human genome rapidly (e.g. in 15 minutes) and at an affordable price (e.g. US \$1000) would be a turning point in medicine. At that price and speed, most people could afford to have their genome sequenced on-the-fly for tailored medical treatment. Thanks to advances in second-generation DNA sequencing techniques, the cost of sequencing an entire human genome is now about US\$ 50,000.<sup>1, 2</sup> However, most second-generation technologies such as those implemented by 454 Life Sciences (Roche), Solexa (Illumina) and Applied Biosystems SOLiD<sup>TM</sup> (Life Technologies), rely on slow iterative cycles of enzymatic processing and imaging-based data collection. Therefore, the most likely candidates to cross the US \$1000 and 15-minute human genome barrier will be third-generation single-molecule sequencing platforms, such as Pacific Bioscience's single molecule-real time sequencing by synthesis (SMRT<sup>TM</sup>) or nanopore sequencing,<sup>3</sup> which are based on the continuous determination of sequences of individual DNA molecules by cycle-free processes.

In one approach to nanopore sequencing, a single-stranded DNA or RNA molecule is driven electrophoretically through a nanopore and each DNA base is read as it passes a recognition point.<sup>3</sup> In its simplest manifestation, the current associated with the passage of ions (e.g. K<sup>+</sup> and Cl<sup>-</sup>) through the nanopore during DNA translocation provides the electrical read-out required to distinguish each base. In our laboratory, we use  $\alpha$ -hemolysin ( $\alpha$ HL) protein nanopores reconstituted in planar lipid bilayers (Figure 1). Notably, we have shown that the four DNA bases,<sup>4-6</sup> including their epigenetically modified forms, 5-methylcytosine and 5-

\*To whom correspondence may be addressed: Department of Chemistry, Catholic University of Leuven, Celestijnenlaan 200G, 3001, Heverlee, Leuven Belgium, giovanni.maglia@chem.kuleuven.be.

<sup>2</sup>Present address: Institute of Bioengineering and Swiss Institute of Experimental Cancer Research, Ecole Polytechnique Fédérale de Lausanne, Lausanne, Switzerland

<sup>3</sup>Present address: Department of Chemistry, University of Leuven, 3001, Heverlee, Leuven, Belgium

hydroxymethylcytosine,<sup>7</sup> can be discriminated in a DNA strand immobilized within the nanopore.

Alternatively, single nucleotides are identified by reading the tunnelling current passing through individual DNA bases, while a DNA strand is translocating through a solid-state nanopore modified with tunnelling probes.<sup>8–10</sup> Tunnelling readings would be advantageous because the nano-ampere range of tunnelling currents will allow the reading of nucleotides at a greater speed than with the pico-ampere ionic currents through protein nanopores.<sup>3</sup> In addition, since the tip of the probe can be less than 1 nm in diameter,<sup>3</sup> a single nucleotide would be addressed by the tunnelling probe at any given time.

One of the main remaining challenges in nanopore sequencing is to reduce the speed of DNA translocation through the nanopore, which is too fast to allow discrimination between individual nucleobases by using either ionic<sup>11</sup> or tunnelling<sup>3</sup> currents. Previous attempts to reduce the speed of free DNA translocation have included the use of low temperatures<sup>12</sup> and increased viscosity<sup>13, 14</sup>. These approaches reduced the speed of DNA translocation by one order of magnitude or less, at the expense of a large decrease in the ionic current. In this work, we show that by lining the transmembrane region of the  $\alpha$ HL pore with positively charged residues, the speed of DNA translocation can be slowed by more than two orders of magnitude. Although, the ionic current during DNA translocation is again almost completely suppressed, we suggest that such nanopores could be used to control the speed of DNA translocation in hybrid protein and solid-state nanopores.

## Ionic currents through $\alpha$ HL nanopores

The heptameric  $\alpha$ HL nanopore contains a cap domain and a barrel domain, which are separated by an inner constriction that is 1.4 nm in diameter (Figure 1).<sup>15</sup> We made a variety of homo- and hetero-heptameric  $\alpha$ HL pores in which the charge distribution within the barrel was altered. In homo-heptamers the mutations appear in all seven subunits, while in hetero-heptamers the charge is changed in a subset of the subunits. All mutants were made by using the RL2 genes as templates, except for the NN<sub>7</sub> pore, in which the WT gene was used (SI). WT pores contain an additional positive charge at position 8 in the form of a lysine residue (Figure 1).

The unitary conductance values ( $g$ ) in 1 M KCl solutions (containing 25 mM Tris.HCl and 100  $\mu$ M EDTA at pH 8.0) varied greatly among the nanopores (Table 1). The introduction of positive charges close to the constriction increased the conductance of the nanopores at positive applied potentials with respect to the WT<sub>7</sub> and RL2<sub>7</sub> pores. By contrast, when positive charges were introduced close to the trans exit of the pore, the ionic current at positive potentials was reduced significantly<sup>16</sup> (Table 1). The rectification ratios ( $g_+/g_-$ ), calculated from the value of the ionic current at +50 mV divided by the current at -50mV, also varied depending on the position of the introduced charges. Nanopores with additional positive charges near the trans exit (after position 121) showed  $g_+/g_- < 1$ , while mutants with positive charges close to the constriction displayed rectifying behaviour similar to that of WT<sub>7</sub> ( $g_+/g_- > 1$ ). On the other hand, NN<sub>7</sub> pores, which have no charged groups at the central constriction, displayed  $g_+/g_- \sim 1$ . In agreement with previous findings,<sup>17–19</sup> these results suggest that the transport of ions through the relatively narrow  $\alpha$ HL nanopore can be strongly influenced by the introduction of charged residues within the  $\beta$  barrel.

## DNA translocation through homo-heptameric $\alpha$ HL nanopores

The addition of a 92mer ssDNA designed to contain no secondary structure (5' - AAAAAAAAAAAAAAAAAAAATTCCCCCCCCCCCCCCCCCTTAAAAAAAAA AAATTCCCCCCCCCTTAAAAAAAAAATTCCCCCCCC-3) to WT<sub>7</sub> and RL2<sub>7</sub>

pores from the cis chamber under positive applied potentials provoked current blockades that are due to the translocation of individual DNA molecules through the pore<sup>20</sup> (Figure 2a). At +120 mV, the most likely translocation time,  $t_p$ , which is defined as the peak of a Gaussian fit to a histogram of translocation times,<sup>12</sup> was  $0.14 \pm 0.01$  ms for both WT<sub>7</sub> and RL2<sub>7</sub> nanopores,<sup>16</sup> corresponding to the mean most likely translocation time per base ( $t_b = t_p / \text{number of nucleotides}$ ) of  $1.5 \mu\text{s/nt}$ .

The manipulation of charges in the barrel of the pore altered the interaction between the DNA and the pore. The addition of one ring of arginine residues near the constriction of RL2 pores (M113R<sub>7</sub>) increased the frequency of DNA translocation by 16-fold.<sup>16</sup> Interestingly, nanopores containing two or more rings of positive charge in the barrel showed only a small additional increase in the frequency of DNA translocation (30% for (M113R-N123)<sub>7</sub>, which was the pore that showed the highest increase, Table 1); indicating that one ring of arginine residues in the barrel is sufficient to enhance the frequency of DNA translocation to near its maximum value.<sup>16</sup>

The removal of the charges at the central constriction in NN<sub>7</sub> or the introduction of one or two rings of arginine residues within the lumen of homo-heptameric RL2 pores (7 or 14 additional positive charges) had only a small effect on the most likely translocation time ( $t_p$ ) for the 92mer or other short ssDNA or RNA molecules.<sup>19, 21</sup> For all double arginine mutants tested (Table 1),  $t_p$  was just 2- or 3- fold higher than the value observed with WT<sub>7</sub> and RL2<sub>7</sub> pores (Table 1). However, the introduction of three (3R<sub>7</sub>) or four (4R<sub>7</sub>) rings of arginine residues within the barrel increased the most likely translocation time by ~10- and ~20-fold, respectively; while seven rings of arginines residues (7R<sub>7</sub>), increased the translocation time by more than two orders of magnitude relative to the WT<sub>7</sub> and RL2<sub>7</sub> values (Table 1). In all the nanopores studied, the translocation times of the current blockades induced by DNA showed a Gaussian distribution followed by an exponential tail (Figure 2b). The most likely translocation time per base decreased exponentially with the applied potential (Figure 2c), confirming that, as for WT<sub>7</sub> pores, individual DNA molecules are translocated through the pore rather than binding and dissociating from the cis side.<sup>22-25</sup>

## Residual currents through homo-heptameric $\alpha$ HL nanopores

When a DNA molecule is translocating through a nanopore, the ionic current is reduced from the open pore current ( $I_O$ ) to the blocked pore current ( $I_B$ ). In WT<sub>7</sub> and RL2<sub>7</sub> nanopores the residual current ( $I_{RES}$ ), defined as  $I_B$  divided by  $I_O$  expressed in percent, is ~10%<sup>16, 20, 26</sup> (Table 1). Modification of the charge distribution within the barrel of the pore has a powerful effect on  $I_{RES}$ . For example, the NN<sub>7</sub> pore, in which the charged residues of the central constriction are substituted by smaller, neutral residues, shows an increased residual current,  $I_{RES}=26\%$  (Table 1), while the introduction of large, positively charged arginine residues greatly reduces  $I_{RES}$  (Table 1). One ring of arginine reduces  $I_{RES}$  to 3%, while three or more sets of arginine residues almost completely suppress the residual current ( $I_{RES} < 1\%$ ).

The effect of arginine substitutions on the residual current during DNA translocation is most likely due to the reduced cross-section of the lumen of the pore, given the increased bulk of the arginine side chains by comparison with the side-chains in WT<sub>7</sub> nanopores,<sup>5</sup> which limit the current flow of hydrated ions through the pore. An additional reduction of the ionic flow is most likely due to the increased electrostatic self-energy of the translocating positive ions (e.g. K<sup>+</sup>)<sup>27, 28</sup> that follows the introduction of the positive charges in the lumen of the pore. Finally, it is also possible that the interaction of the positive charges of the arginine side chains with the backbone phosphates of DNA<sup>29</sup> triggers a partial collapse of the  $\beta$  barrel around the DNA, which in turn prevents the passage of ions through the pore.

## DNA translocation through $\alpha$ HL hetero-heptameric pores

Hetero-heptameric  $\alpha$ HL pores were prepared by mixing 7R-monomers containing an eight-aspartate tail (D8) at the C terminus with RL2-monomers, followed by separation by SDS-PAGE (SI). When incorporated into heptamers, each 7R monomers provides seven arginine residues within the barrel (starting from the constriction and ending at the trans exit of the pore). It was hoped that the arginine side chains would interact with the phosphodiester linkages of DNA and reduce the rate of translocation, while the relatively small side-chains of the RL2-subunits would still allow the passage of a significant ionic current.

We found that hetero-heptameric pores containing 7R monomers were as efficient as homopolymeric pores containing arginine residues at reducing the rate of translocation of DNA through the pore (Figure 4 and Table 1), with the translocation times per base showing an exponential dependence on the number of arginine residues in the barrel (Figure 4). Unfortunately,  $I_{RES}$  was again reduced to almost zero when 21 or more arginine residues were introduced into the barrel of the pore (table 1).

## Conclusions

In this work, we have shown that molecular brakes in the form of additional positive charge can be engineered within the barrel of a protein nanopore to control the average speed of translocation of a short ssDNA molecule containing no secondary structure. Although the introduction of more than two positively charged residues per subunit in homo-heptamers or more than two 7R subunits in hetero-heptamers largely prevented the passage of ions through the pore, the results obtained here may still be useful for the implementation of nanopore sequencing platforms. For example, an artificial barrel containing positive charges could be paired with a pore capable of base recognition (e.g. NN<sub>7</sub>).<sup>4</sup> The charge within the artificial barrel would be used to control DNA translocation, while the trans-membrane pore would recognize single DNA bases (Figure 5a). In such a construct, we believe that substantial current will flow, as previous studies have shown that proteins handling DNA placed at the cis entrance to the  $\alpha$ HL nanopore do not drastically alter the ionic current through the pore and allow bases to be discriminated<sup>4, 30–32</sup>

Alternatively, modified  $\alpha$ HL pores could be inserted into solid-state nanopores<sup>33</sup> paired with suitable tunnelling probes<sup>34–37</sup> (Figure 5b). The feasibility of this approach has been described theoretically<sup>38–42</sup> and the ability of scanning tunnelling microscopy to recognize single bases has been shown experimentally.<sup>43–45</sup> However, in order to be identified during translocation through a nanopore, each DNA base would have to be addressed by the tunnelling probes for at least 100  $\mu$ s,<sup>3</sup> which is three orders of magnitude longer than the typical average translocation times of individual DNA bases or base pairs through solid state nanopores.<sup>3, 46–48</sup> In addition, a reproducible orientation and positioning of the base at the tunneling probe will also be crucial, as electron-tunneling currents are exponentially sensitive to atomic scale changes of orientation and distance.<sup>3</sup> Therefore, if tunnelling probes will be incorporated into solid-state nanopores with atomic precision, the hybrid protein and solid-state nanopore systems shown in figure 5b will be capable of informative data acquisition ( $t_b = 270 \mu$ s/base at +120mV), providing that the speed of DNA translocation through the pore is constant and the orientation of each base at the tunnelling probe reproducible.<sup>3</sup>

## Acknowledgments

We are grateful to David Stoddart and to Gabriel Villar for proof reading and insightful comments and for helping with data fitting. This work was funded by the National Institutes of Health.

## References

1. Drmanac R, Sparks AB, Callow MJ, Halpern AL, Burns NL, Kermani BG, Carnevali P, Nazarenko I, Nilsen GB, Yeung G, Dahl F, Fernandez A, Staker B, Pant KP, Baccash J, Borcharding AP, Brownley A, Cedeno R, Chen L, Chernikoff D, Cheung A, Chirita R, Curson B, Ebert JC, Hacker CR, Hartlage R, Hauser B, Huang S, Jiang Y, Karpinchyk V, Koenig M, Kong C, Landers T, Le C, Liu J, McBride CE, Morenzoni M, Morey RE, Mutch K, Perazich H, Perry K, Peters BA, Peterson J, Pethiyagoda CL, Pothuraju K, Richter C, Rosenbaum AM, Roy S, Shafto J, Sharanovich U, Shannon KW, Sheppy CG, Sun M, Thakuria JV, Tran A, Vu D, Zaranek AW, Wu X, Drmanac S, Oliphant AR, Banyai WC, Martin B, Ballinger DG, Church GM, Reid CA. *Science*. 2010; 327(5961):78–81. [PubMed: 19892942]
2. Bonetta L. *Cell*. 2010; 141(6):917–9. [PubMed: 20550926]
3. Branton D, Deamer DW, Marziali A, Bayley H, Benner SA, Butler T, Di Ventra M, Garaj S, Hibbs A, Huang X, Jovanovich SB, Krstic PS, Lindsay S, Ling XS, Mastrangelo CH, Meller A, Oliver JS, Pershin YV, Ramsey JM, Riehn R, Soni GV, Tabard-Cossa V, Wanunu M, Wiggin M, Schloss JA. *Nature Biotechnology*. 2008; 26:1146–1153.
4. Stoddart D, Heron A, Mikhailova E, Maglia G, Bayley H. *Proc Natl Acad Sci USA*. 2009; 106:7702–7707. [PubMed: 19380741]
5. Stoddart D, Heron AJ, Klingelhofer J, Mikhailova E, Maglia G, Bayley H. *Nano Lett*. 2010; 10(9):3633–7. [PubMed: 20704324]
6. Stoddart D, Maglia G, Mikhailova E, Heron AJ, Bayley H. *Angewandte Chemie-International Edition*. 2010; 49(3):556–559.
7. Wallace EV, Stoddart D, Heron AJ, Mikhailova E, Maglia G, Donohoe TJ, Bayley H. *Chem Commun (Camb)*. 46(43):8195–7. [PubMed: 20927439]
8. Zwolak M, Di Ventra M. *Nano Letters*. 2005; 5(3):421–424. [PubMed: 15755087]
9. Zikic R, Krstic PS, Zhang XG, Fuentes-Cabrera M, Wells J, Zhao XC. *Physical Review E*. 2006; 74(1)
10. Lagerqvist J, Zwolak M, Di Ventra M. *Nano Letters*. 2006; 6(4):779–782. [PubMed: 16608283]
11. Deamer D. *Annu Rev Biophys*. 2010; 39:79–90. [PubMed: 20192777]
12. Meller A, Nivon L, Brandin E, Golovchenko J, Branton D. *Proc Natl Acad Sci U S A*. 2000; 97(3):1079–84. [PubMed: 10655487]
13. Kawano R, Schibel AE, Cauley C, White HS. *Langmuir*. 2009; 25(2):1233–7. [PubMed: 19138164]
14. Fologea D, Uplinger J, Thomas B, McNabb DS, Li J. *Nano Lett*. 2005; 5(9):1734–7. [PubMed: 16159215]
15. Song L, Hobaugh MR, Shustak C, Cheley S, Bayley H, Gouaux JE. *Science*. 1996; 274(5294):1859–66. [PubMed: 8943190]
16. Maglia G, Rincon Restrepo M, Mikhailova E, Bayley H. *Proc Natl Acad Sci U S A*. 2008; 105:19720–19725. [PubMed: 19060213]
17. Gu LQ, Cheley S, Bayley H. *Proc Natl Acad Sci U S A*. 2003; 100(26):15498–503. [PubMed: 14676320]
18. Maglia G, Heron AJ, Hwang WL, Holden MA, Mikhailova E, Li Q, Cheley S, Bayley H. *Nat Nanotechnol*. 2009; 4(7):437–40. [PubMed: 19581896]
19. Maglia M, Henricus M, Wyss R, Li Q, Cheley S, Bayley H. *Nano Letters*. 2009; 9:3831–3836. [PubMed: 19645477]
20. Kasianowicz JJ, Brandin E, Branton D, Deamer DW. *Proc Natl Acad Sci U S A*. 1996; 93(24):13770–3. [PubMed: 8943010]
21. Japrun D, Henricus M, Li QH, Maglia G, Bayley H. *Biophysical Journal*. 2010; 98(9):1856–1863. [PubMed: 20441749]
22. Clarke J, Wu H, Jayasinghe L, Patel A, Reid S, Bayley H. *Nature Nanotechnology*. 2009; 4:265–270.
23. Braha O, Webb J, Gu LQ, Kim K, Bayley H. *Chemphyschem*. 2005; 6(5):889–92. [PubMed: 15884071]

24. Gu LQ, Cheley S, Bayley H. *Science*. 2001; 291(5504):636–40. [PubMed: 11158673]
25. Sanchez-Quesada J, Ghadiri MR, Bayley H, Braha O. *Journal of the American Chemical Society*. 2000; 122(48):11757–11766.
26. Meller A. *J Phys: Condens Matter*. 2003; 15:R581–R607.
27. Bonthuis DJ, Zhang J, Hornblower B, Mathe J, Shklovskii BI, Meller A. *Phys Rev Lett*. 2006; 97(12):128104. [PubMed: 17026003]
28. Zhang J, Shklovskii BI. *Phys Rev E Stat Nonlin Soft Matter Phys*. 2007; 75(2 Pt 1):021906. [PubMed: 17358366]
29. Cheley S, Gu L-Q, Bayley H. *Chem Biol*. 2002; 9:829–838. [PubMed: 12144927]
30. Derrington IM, Butler TZ, Collins MD, Manrao E, Pavlenok M, Niederweis M, Gundlach JH. *Proc Natl Acad Sci U S A*. 2010; 107(37):16060–5. [PubMed: 20798343]
31. Cockroft SL, Chu J, Amarin M, Ghadiri MR. *J Am Chem Soc*. 2008; 130(3):818–20. [PubMed: 18166054]
32. Olasagasti F, Lieberman KR, Benner S, Cherf GM, Dahl JM, Deamer DW, Akeson M. *Nat Nanotechnol*. 2010; 5(11):798–806. [PubMed: 20871614]
33. Hall Scott A, Rotem D, Mehta K, Bayley H, Dekker C. *Nature Nanotechnology*. 2011 In press.
34. Taniguchi M, Tsutsui M, Yokota K, Kawai T. *Applied Physics Letters*. 2009; 95(12):123701.
35. Ivanov AP, Instuli E, McGilvery C, Baldwin G, McComb DW, Albrecht T, Edel JB. *Nano Lett*.
36. Gierhart BC, Howitt DG, Chen SJ, Zhu Z, Kotecki DE, Smith RL, Collins SD. *Sens Actuators B Chem*. 2008; 132(2):593–600. [PubMed: 19584949]
37. Fischbein MD, Drndic M. *Nano Lett*. 2007; 7(5):1329–37. [PubMed: 17439186]
38. Lagerqvist J, Zwolak M, Di Ventra M. *Phys Rev E Stat Nonlin Soft Matter Phys*. 2007; 76(1 Pt 1): 013901. author reply 013902. [PubMed: 17677520]
39. Krems M, Zwolak M, Pershin YV, Di Ventra M. *Biophys J*. 2009; 97(7):1990–6. [PubMed: 19804730]
40. Lagerqvist J, Zwolak M, Di Ventra M. *Biophys J*. 2007; 93(7):2384–90. [PubMed: 17526560]
41. Lagerqvist J, Zwolak M, Di Ventra M. *Nano Lett*. 2006; 6(4):779–82. [PubMed: 16608283]
42. Zwolak M, Di Ventra M. *Nano Lett*. 2005; 5(3):421–4. [PubMed: 15755087]
43. Ohshiro T, Umezawa Y. *Proc Natl Acad Sci U S A*. 2006; 103(1):10–4. [PubMed: 16373509]
44. He J, Lin L, Zhang P, Lindsay S. *Nano Lett*. 2007; 7(12):3854–8. [PubMed: 18041859]
45. Tanaka H, Kawai T. *Nat Nanotechnol*. 2009; 4(8):518–22. [PubMed: 19662015]
46. Storm AJ, Storm C, Chen J, Zandbergen H, Joanny JF, Dekker C. *Nano Lett*. 2005; 5(7):1193–7. [PubMed: 16178209]
47. Fologea D, Gershow M, Ledden B, McNabb DS, Golovchenko JA, Li J. *Nano Lett*. 2005; 5(10): 1905–9. [PubMed: 16218707]
48. Li J, Gershow M, Stein D, Brandin E, Golovchenko JA. *Nat Mater*. 2003; 2(9):611–5. [PubMed: 12942073]



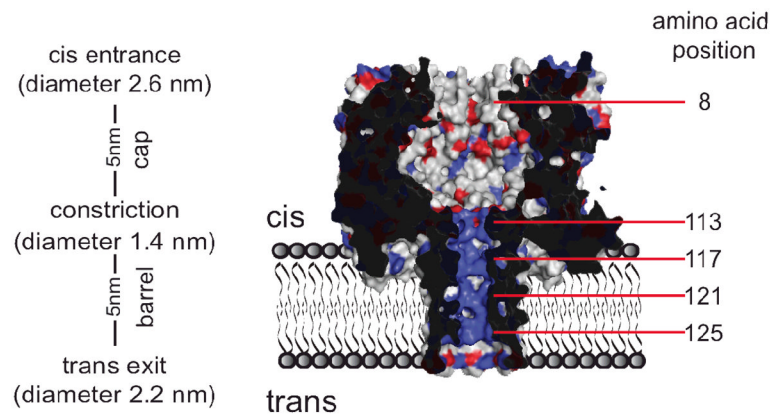


**Figure 1.**

Section through a 7R<sub>7</sub> nanopore. The amino acids at positions 113, 115, 117, 119, 121, 123 and 125 were replaced in the WT<sub>7</sub> nanopore (PDB:7AHL) by arginine by using PyMOL software (DeLano Scientific LLC, v1.0). 7R<sub>7</sub> is in the RL2 background, in which lysine 8 is replaced by alanine as shown here. Negatively charged residues are colored in red and positively charged residues in blue.

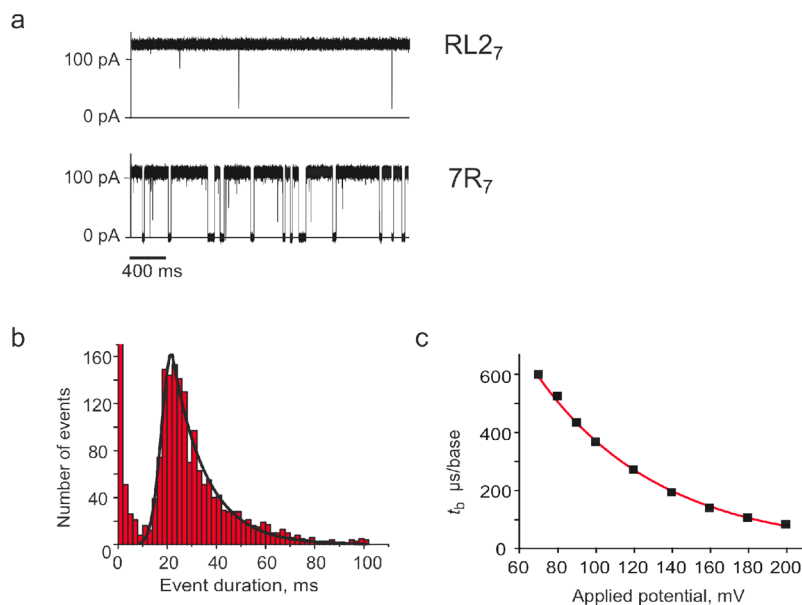


**Figure 2.** DNA translocation through 7R<sub>7</sub> nanopores. a) Single-channel recordings of RL2<sub>7</sub> (top) and 7R<sub>7</sub> nanopores (bottom) at +120 mV after the addition of 1.0  $\mu$ M 92-mer ssDNA to the cis compartment. b) Event histogram showing the translocation time distribution at +120 mV through a 7R<sub>7</sub> pore upon addition of 0.7  $\mu$ M ssDNA (92-mer) to the cis compartment. Events of < 10 ms are attributed to the transient gating of the 7R<sub>7</sub> nanopore and are ignored (Figure S1). The solid line shows a fit to the histogram of a Gaussian followed by a single exponential.<sup>12</sup> The most likely translocation time ( $t_b$ ) is defined by the peak of the Gaussian fit.<sup>12</sup> c) Dependence on the applied voltage of the most likely translocation time per base ( $t_b = t_p / 92$ ) of ssDNA (92 mer) through 7R<sub>7</sub> nanopores. The red line shows a single exponential fit. Experiments were performed in 1 M KCl, 25 mM Tris.HCl, containing 100  $\mu$ M EDTA, at pH 8.0.



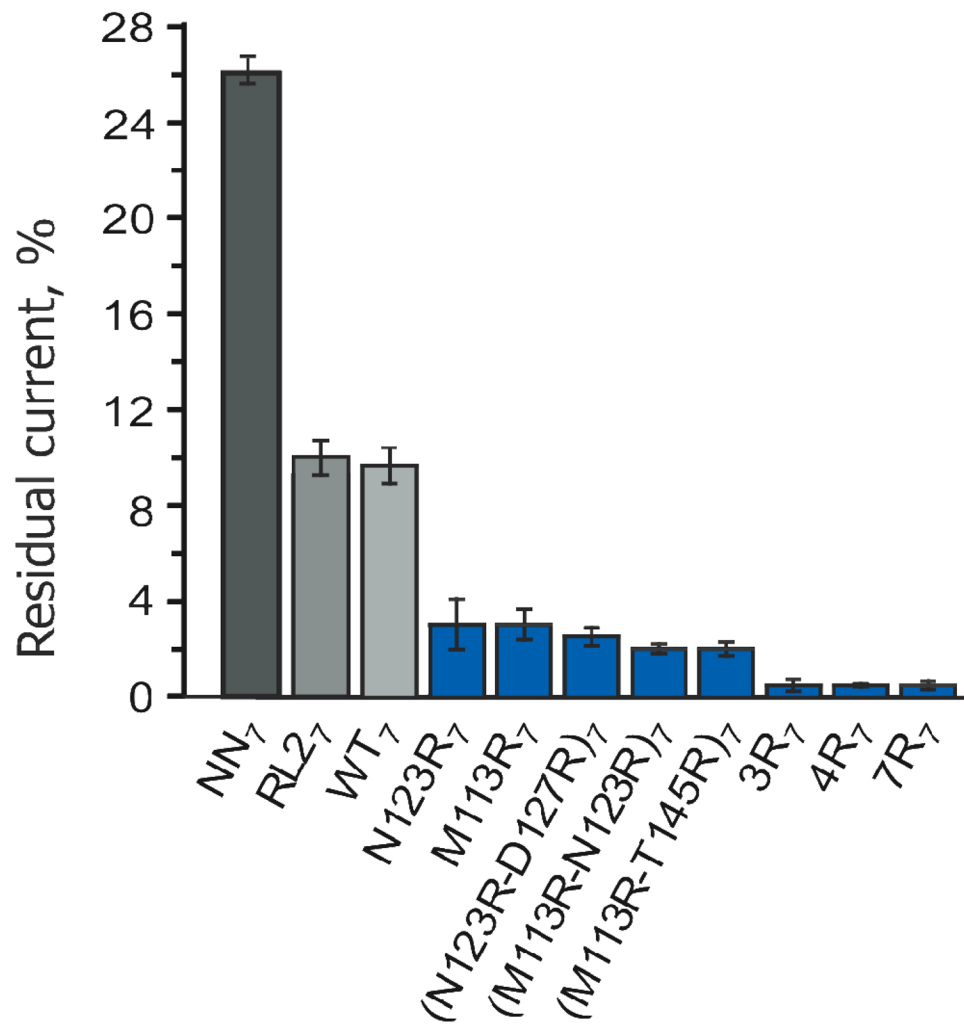


**Figure 3.** Residual current ( $I_{RES}$ ) through  $\alpha$ HL nanopores during ssDNA translocation at +120 mV. Errors are expressed as standard deviations. All nanopores, except WT<sub>7</sub> and NN<sub>7</sub>, are in the RL2<sub>7</sub> background. Nanopores with additional positive charge compared to the WT<sub>7</sub> and RL2<sub>7</sub> pores are in blue. Experiments were performed in 1 M KCl, 25 mM Tris.HCl, containing 100  $\mu$ M EDTA, at pH 8.0.

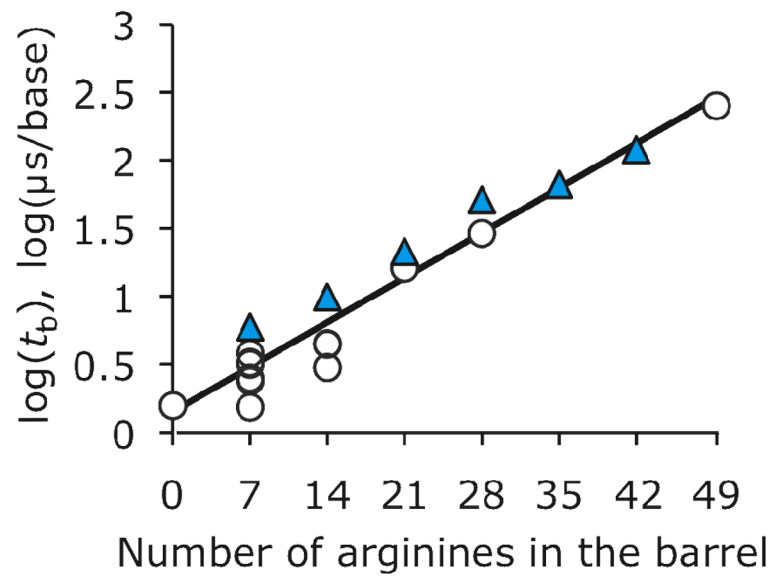


**Figure 4.** Dependence of the mean most likely translocation time per base ( $t_b$ ) at +120 mV on the number of arginine residues in the barrel of RL2 pores. Homo- and hetero-heptamers are shown in open circles and blue triangles, respectively.  $t_b$  is expressed on a logarithmic scale and the data are fitted to a linear regression. Hetero-heptamers were obtained by mixing RL2- and 7R- monomers. Experiments were performed in 1 M KCl, 25 mM Tris.HCl, containing 100  $\mu\text{M}$  EDTA, at pH 8.

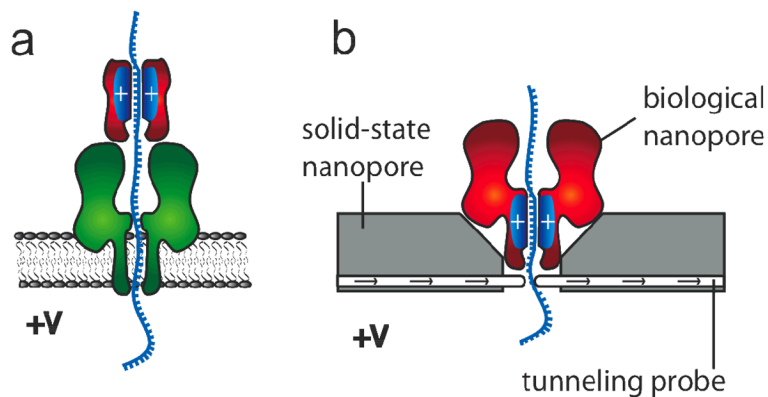


**Figure 5.** Potential uses of 7R<sub>7</sub> nanopores. a) A protein nanopore (e.g. NN<sub>7</sub>, green) is used to detect base-specific ionic current differences in a DNA strand, while a synthetic protein barrel (red) containing positive charges is employed to control the speed of DNA translocation. b) A protein nanopore with positive internal charge (e.g. 7R<sub>7</sub>, red) is paired with a solid-state nanopore (gray) equipped with a tunnelling probe integrated into the device with atomic precision. The speed at which DNA is translocated through the solid-state nanopore is controlled by the applied potential and the number of positive charges in the barrel of the protein nanopore. Each base will be read by monitoring the tunnelling current, providing that the bases translocate at a constant speed and arrive with the same orientation at the tunnelling probe.

**Table 1**

DNA translocation through  $\alpha$ HL nanopores at +120 mV in 1 M KCl, 25 mM Tris.HCl containing 100  $\mu$ M EDTA at pH 8.0.  $t_b$  is the most likely DNA translocation time per base;  $f$  is the normalized frequency of DNA translocation;  $g$  is the unitary conductance and  $I_{RES}$  is the residual current during DNA translocation. For  $I_{RES}$ , the errors were all less than  $\pm 1\%$ . All mutants, except NN<sub>7</sub>, are in the RL2 background (WT pores contain an additional positive charge at position 8 in the form of a lysine residue, SI). Errors are shown as standard deviations.

Pore	$t_b$ ( $\mu$ s/base)	$f$ ( $s^{-1}\mu$ M <sup>-1</sup> )	$I_{RES}$ (%)	$g$ , nS (+120mV)
WT <sub>7</sub>	1.5 $\pm$ 0.1 (n=6)	3.0 $\pm$ 0.2 (n=12)	10 (n=5)	1.01 $\pm$ 0.01 (n=23)
NN <sub>7</sub> (E111N-K147N)	2.0 $\pm$ 0.1 (n=4)	0.79 $\pm$ 0.12 (n=4)	26 (n=4)	1.07 $\pm$ 0.05 (n=4)
RL2 <sub>7</sub>	1.6 $\pm$ 0.1 (n=4)	0.28 $\pm$ 0.04 (n= 5)	10 (n=4)	1.03 $\pm$ 0.02 (n=16)
M113R <sub>7</sub>	1.5 $\pm$ 0.1 (n=4)	4.4 $\pm$ 0.6 (n=7)	3 (n=5)	1.17 $\pm$ 0.02 (n=8)
N123R <sub>7</sub>	2.4 $\pm$ 0.5 (n=5)	0.43 $\pm$ 0.04 (n= 8)	3 (n=4)	0.64 $\pm$ 0.02 (n=10)
(M113R-N123) <sub>7</sub>	3.0 $\pm$ 0.3 (n=8)	6.2 $\pm$ 1.9 (n=7)	2 (n=4)	0.97 $\pm$ 0.05 (n=6)
(N123R-D127R) <sub>7</sub>	4.4 $\pm$ 0.2 (n=5)	0.4 $\pm$ 0.05 (n=4)	2 (n=5)	0.57 $\pm$ 0.03 (n=4)
(M113R-T145R) <sub>7</sub>	4.5 $\pm$ 0.7 (n=5)	5.2 $\pm$ 1.0 (n=5)	2 (n=5)	1.06 $\pm$ 0.06 (n=5)
3R <sub>7</sub> (T115R, G119R, N123R) <sub>7</sub>	16 $\pm$ 4 (n=7)	4.2 $\pm$ 1.4 (n=5)	<1 (n=6)	0.87 $\pm$ 0.06 (n=7)
4R <sub>7</sub> (T115R, G119R, N123R, D127R) <sub>7</sub>	29 $\pm$ 6 (n=4)	3.5 $\pm$ 3.5 (n=4)	<1 (n=4)	0.70 $\pm$ 0.09 (n=6)
7R <sub>7</sub> (M113R-T115R-T117R- G119R-N121R-N123R- T125R) <sub>7</sub>	270 $\pm$ 10 (n=6)	5.4 $\pm$ 1.6 (n=6)	<1 (n=6)	0.91 $\pm$ 0.04 (n=10)
7R <sub>6</sub> RL2 <sub>1</sub>	120 $\pm$ 10 (n=7)	1.54 $\pm$ 0.5 (n=6)	<1 (n=5)	0.95 $\pm$ 0.06 (n=7)
7R <sub>5</sub> RL2 <sub>2</sub>	67 $\pm$ 10 (n=5)	3.5 $\pm$ 0.8 (n=4)	<1 (n=5)	0.88 $\pm$ 0.09 (n=5)
7R <sub>4</sub> RL2 <sub>3</sub>	51 $\pm$ 6 (n=5)	3.3 $\pm$ 0.7 (n=5)	<1 (n=5)	0.87 $\pm$ 0.05 (n=5)
7R <sub>3</sub> RL2 <sub>4</sub>	21 $\pm$ 9 (n=7)	4.0 $\pm$ 1.5 (n=7)	1 (n=5)	0.94 $\pm$ 0.05 (n=7)
7R <sub>2</sub> RL2 <sub>5</sub>	9.9 $\pm$ 2.2 (n=5)	2.3 $\pm$ 0.5 (n=4)	2 (n=5)	0.93 $\pm$ 0.07 (n=5)
7R <sub>1</sub> RL2 <sub>6</sub>	6.0 $\pm$ 1.1 (n=5)	1.7 $\pm$ 0.3 (n=5)	4 (n=4)	0.99 $\pm$ 0.05 (n=5)